Electronic Supplementary Material (ESI) for Soft Matter.
This journal is © The Royal Society of Chemistry 2020

Supplementary Information

Micellar Structure and Transformations in Sodium Alkylbenzenesulfonate (NaLAS) Aqueous Solutions: Effects of Concentration, Temperature and Salt

Aysha S. Rafique[a], Sepideh Khodaparast[a,†], Andreas S. Poulos[a], William N. Sharratt[a], Eric S. J. Robles[b], and João T. Cabral[a,*]

[a] Department of Chemical Engineering, Imperial College London, London, SW7 2AZ, U.K.
[b] The Procter & Gamble Company, Newcastle Innovation Centre, Newcastle-Upon-Tyne, NE12 9TS, U.K.
[†] Present address: School of Mechanical Engineering, University of Leeds, Leeds, LS2 9JT, U.K.
[*] j.cabral@imperial.ac.uk

1 Reproducibility and batch variability

Two batches of NaLAS were independently tested in 2016 and 2018. Pure NaLAS solutions prepared from different batches were tested to ensure reproducibility of measurements, see Fig. S1. Small variations in SANS data presented in Fig. S1 may be attributed to the NaLAS concentration and compound variations in different batches, uncertainties in sample preparation, and data reduction.

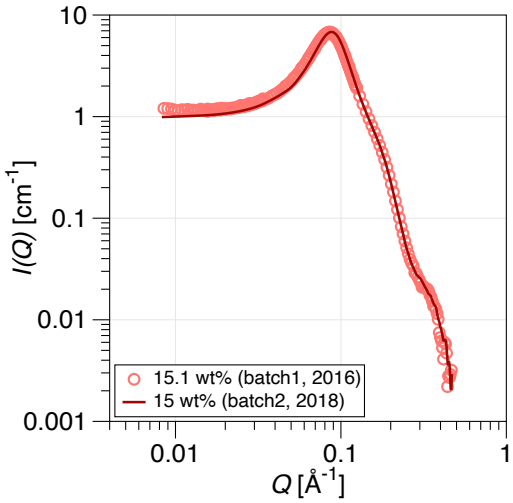

Figure S1. Comparison between independent SANS measurements performed on two different batches of NaLAS.

Although small variations in concentration of NaLAS and its components are expected in various batches, trends in micellar shape, size, and transformations reported here were generally reproducible. Fig. S2a,b compare independent SANS measurements performed on two different batches of NaLAS. Note that the H_2O/D_2O matrix compositions varies slightly between both sets of experiments, thereby impacting the incoherent background and contrast factor, and thus the overall scattering intensity. At lower NaLAS concentrations (here 0.5 and 0.6 wt%), similar micellar phases and transformations to MLVs were detected in both measurements. Small variations in concentration of batches and sample preparation may lead to minor detectable features in the results, however, our measurements on solutions of significantly different concentrations of NaLAS showed presence of similar transformations from spherical to cylindrical micelles and the formation of MLVs at higher concentration of salt, see Fig. S2c,d. Transformation to MLVs was generally enhanced at lower salt concentrations in solutions with a larger content of NaLAS. Similarly, we expect the impact of temperature modification to be qualitatively reproducible in various batches with minor quantitative differences due to variation in content and concentration of NaLAS.

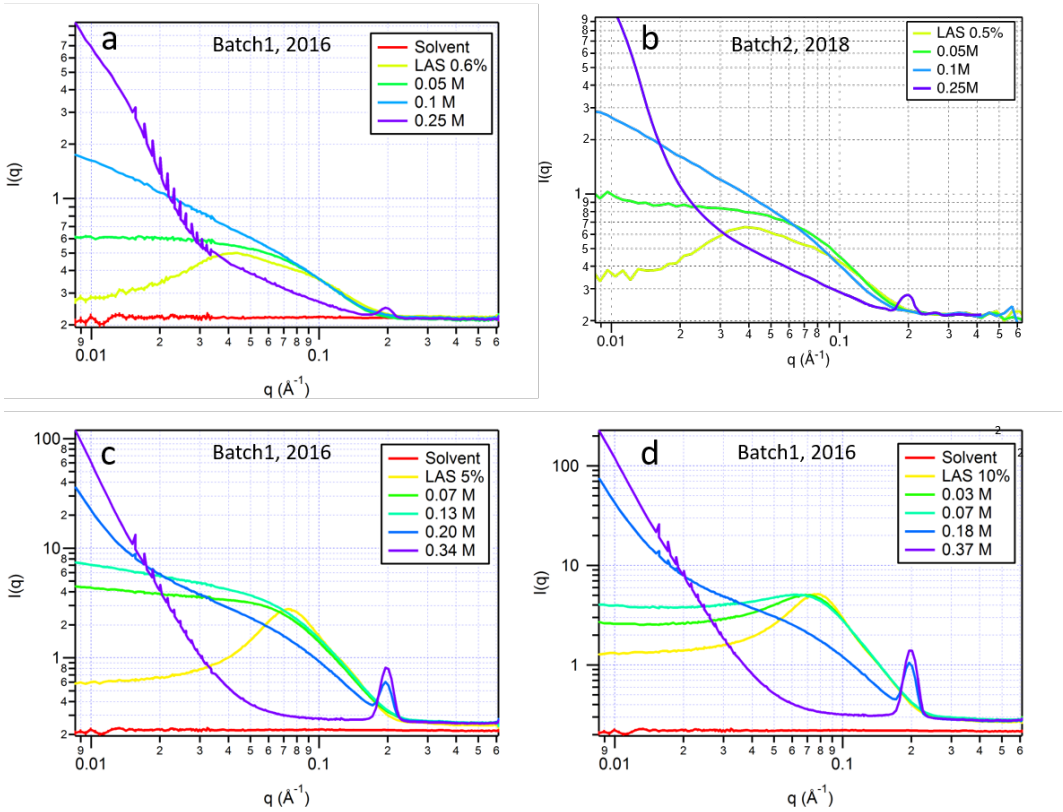

Figure S2. Reproducibility of SANS measurements for different batches of NaLAS. (a) and (b) show independent SANS measurements performed in 2016 and 2018 on two different batches. Similar micellar solutions and transformation to MLVs were found for both batches. (c) and (d) Micellar transformation and MLV formation at higher concentrations of NaLAS.

2 Dynamic light scattering

DLS measurements were carried out using a Zetasizer Nano Z (Malvern Panalytical) equipped with a He-Ne laser in backscattering geometry. To account for the double decay observed in the data, the correlation functions were fitted to:

$$g^{(1)}(\tau) = Ae^{-2\tau(\frac{\Gamma}{R_{h1}})} + Be^{-2\tau(\frac{\Gamma}{R_{h2}})} \quad (1)$$

where $\Gamma = D_0 Q^2$ and D_0 is a translational diffusion coefficient, related to the hydrodynamic radius (R_h) by the Stokes-Einstein relation:

$$R_h = \frac{k_B T}{3\pi\eta D_0} \quad (2)$$

where k_B is the Boltzmann constant, T is temperature (K) and η is solvent viscosity (water, 0.887 mPa.s). Our measurements were carried out at θ = 173 °and λ = 633 nm, and refractive index n that varied with increasing salt concentration (0.01 M Na_2SO_4: n = 0.892; 0.3 M Na_2SO_4: n = 1.05). The resulting wavenumber $Q = (4\pi n/\lambda)sin(\theta/2)$ ranged from 0.0177 nm^{-1} (0.01 M Na_2SO_4) to 0.0208 (0.3 M Na_2SO_4). For illustration, the correlation data obtained for a solution of 0.5 wt% NaLAS and 0.1 M Na_2SO_4 indicated two discrete particle sizes of R_{h1} = 1.9 nm and R_{h2} = 85 nm, with prefactors of A = 0.93 and B = 0.07, respectively. Given the small contribution and larger uncertainty of the latter, focus on the first population and report R_{h1} as an *apparent* R_h (given that micelle shape deviates from sphericity and become highly elongated), for all samples in investigated.

3 Scattering Length Density (SLD) calculation

The aqueous NaLAS micellar system was fitted using an ellipsoid core-shell model for the form factor and the Hayter-Penfold rescaled mean spherical approximation (RMSA) to model the structure factor. The ternary NaLAS-Na_2SO_4-H_2O system was similarly fitted using a cylinder core shell model. The scattering length densities (SLDs) are calculated from the sum of the scattering lengths of atoms present in each subsection of an NaLAS molecule divided by the volume of the subsection. To calculate the overall molecular volume we assumed two alkyl terminal methyl groups are present in the alkyl chain and used cited volumes for -CH_2 (26.9 Å) and -CH_3 (54.8 Å).[1] As shown in Fig. S3, we consider the shell to comprise the surfactant headgroup (sodium benzenesulfonate) and the core as the alkyl chain in pure NaLAS micelles. The maximum dimensions of the alkyl chain in the micellar core (l_c) is calculated using Tanford's relation:[1]

$$l_c = 2.765 + 1.265n$$

where n is the number of -CH_2 groups within the chain. The headgroup volume was calculated using C-C bond lengths present in benzene (1.4 Å) and the sulfonate anion as given by Hayter and Penfold (60.4 Å).[2] Our calculations yield an initial value of SLD_{core} = -0.443 $\times 10^{-6}$ Å^{-2} and SLD_{shell} = 1.69 $\times 10^{-6}$ Å^{-2} to provide a micellar fit comprising r_{core} = 15 Å and t_{shell} = 5 Å for the aqueous micellar solution of NaLAS. Fig. S4 is an illustration of the NaLAS micellar structure in D_2O with the associated SLDs.

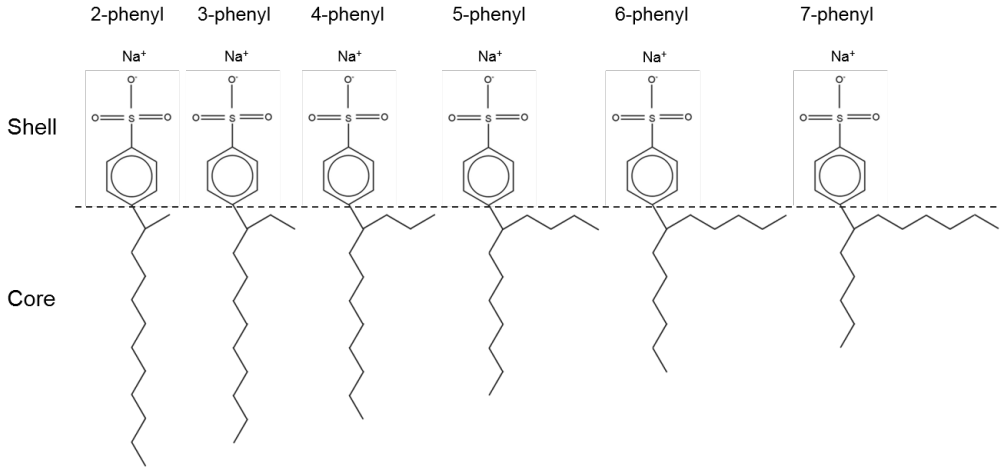

Figure S3. Schematic detailing the chemical structures of the core and shell components considered in the shell model fitted to SANS data. Various phenyl isomers of NaLAS with a C12 chain are displayed.

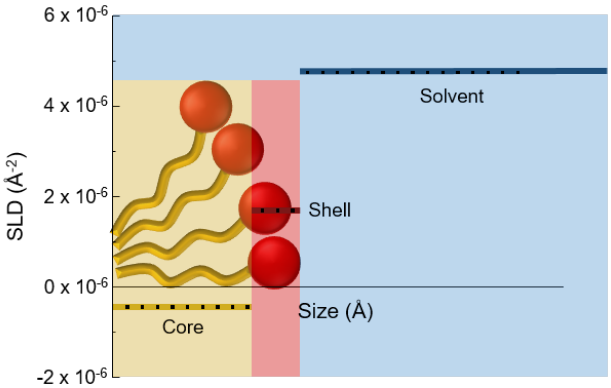

Figure S4. Schematic of the SLD profile of NaLAS core-shell micelles within a D_2O matrix (solvent).

During our fitting procedure, SLD values were left as free parameters. The calculated SLD values were used as initial values. Increasing concentration of NaLAS in binary mixtures was found to have negligible effect on the SLD values obtained, see Fig. S5.

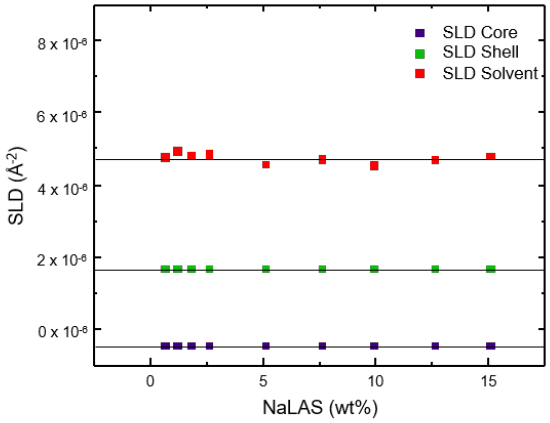

Figure S5. SLD values obtained through the fitting procedure for binary solutions of NaLAS at various concentrations.

Starting from SLD estimations for binary solutions of NaLAS, fitting the SANS data for ternary NaLAS/Na_2SO_4/water solutions yield small changes to the SLD_{shell} and $SLD_{solvent}$, respectively, while the SLD_{core} remained relatively invariant, see Fig. S6. These small changes in SLD likely reflect limitations in the applicability of the core-shell model and mean-field interactions, possible variations in hydration and polydispersity, in the micelle-monomer equilibrium associated with a shift in CMC, or in the partial molar volume and micellar aggregation number, impacting the contrast factor and overall intensity of the scattering.

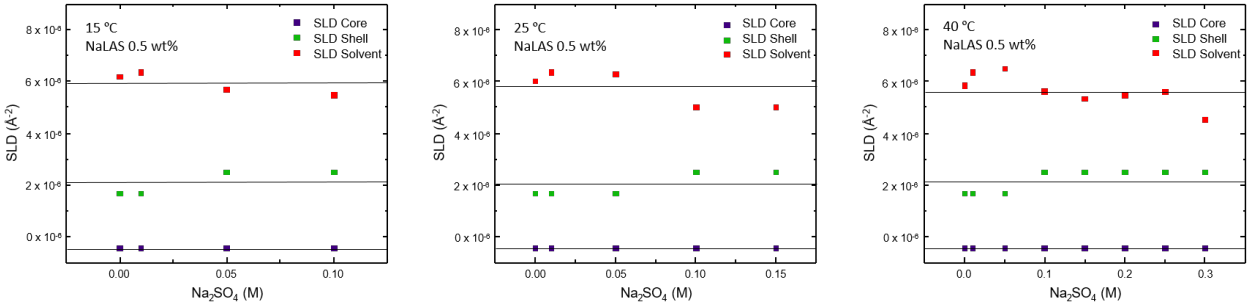

Figure S6. SLD values obtained through the fitting procedure for ternary NaLAS/Na_2SO_4/water solutions at various temperatures.

4 Structure factor $S(Q)$ for NaLAS aqueous solutions estimated by SANS

SANS measurements of aqueous micellar solutions of NaLAS were analysed to estimate an $S(Q)$ as a function of concentration. The calibrated scattering intensity was normalised by the volume concentration of NaLAS (Φ) and the (mostly incoherent) background was subtracted using: $I_{corr} = (I - background)/\Phi$. The structure factor $S(Q)$ was subsequently obtained by dividing each scattering profile by the form factor $P(Q)$, shown in Fig.S7.

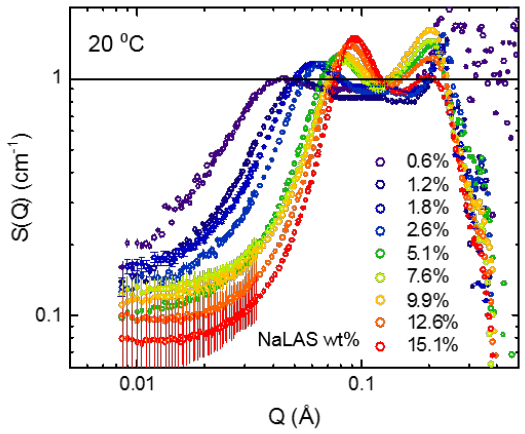

Figure S7. Structure factor $S(Q)$ experimentally obtained by SANS data of aqueous micellar solutions of NaLAS at different concentrations at 20 °C. The structure factor ($S(Q)$) was estimated by $S(Q) = I_{corr}(Q)/P(Q)$

Fig. S8 shows the peak locations obtained from the total scattering intensity $I(Q)$, as well as from the structure factor $S(Q)$, as a function of NaLAS concentration. Both sets of data show similar trends, corroborating the qualitative assertion made based on Q_{peak} data shown in Fig. 2b of the main paper.

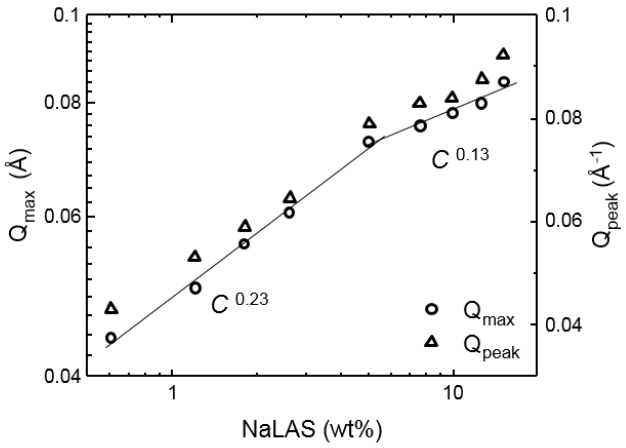

Figure S8. Wavenumber Q associated with the maximum scattering intensity $I(Q)$ (obtained from Fig. 2(a)), termed Q_{max} and shown by open circles, as well as with the first peak in $S(Q)$, Q_{peak} (obtained from Fig. S7) shown by open triangles, as a function of concentration of NaLAS wt%. The power law exponents are discussed in the main text.

5 Additional SANS data for 0.5% NaLAS with added salt, at T=15, 40 °C

Aqueous micellar NaLAS aggregates are found to be spherical with a core radius of 15 Å and a shell thickness of 5 Å. With the addition of electrolyte the micelles elongate with salt concentration, with higher temperatures promoting the formation of longer cylindrical micelles. At a threshold Na_2SO_4 concentration the cylindrical micelles form MLVs, and this threshold value also increases with temperature. SANS data for T=15 and 40 °C, as well as model fits, are provided in Fig. S9, complementing the data fits at T=25 °C, included in the main paper.

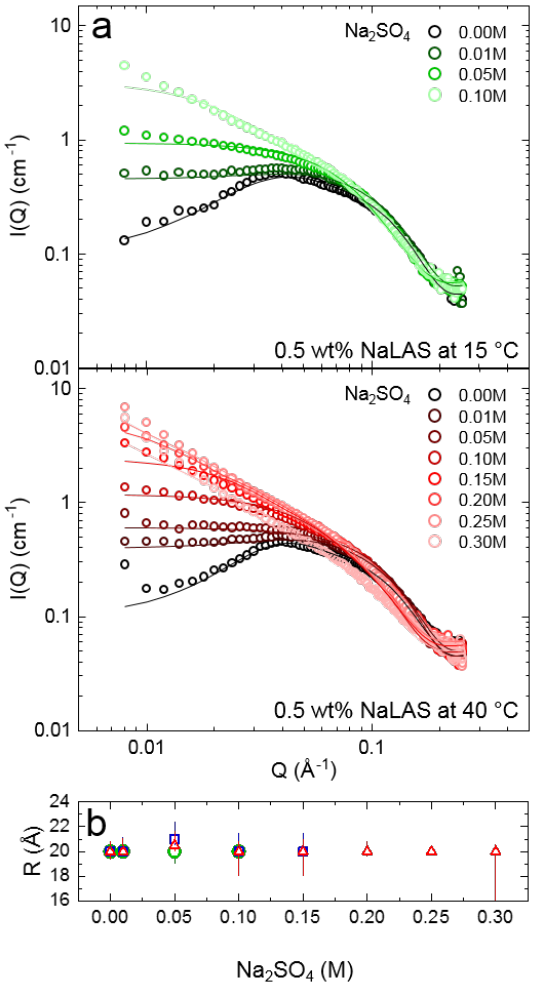

Figure S9. Elongation of NaLAS micelles with addition of salt. (a) Experimental SANS data for 0.5 wt% NaLAS at 15 °C (containing Na_2SO_4 concentrations varying from 0-0.1 M) and at 40 °C (containing Na_2SO_4 concentrations varying from 0-0.3 M) in open circles with fitted data superimposed. (b) Fitted data indicate that the microstructure is initially made up of spherical micelles which elongate with increasing salt concentration, while the radius remains approximately constant.

6 Micellar charge obtained from SANS data fitting

Salt addition results in increased micellar charge screening, which then enables the series of micellar transformations described in the main paper. SANS data fitting[2] indicates that the surface charge of each micelle particle becomes progressively less negative, and then decreases rapidly at a threshold salt concentration, shown in Fig. S10. This salt concentration also corresponds to the phase transformation from spherical micelles to cylindrical micelles, where the low Q power law exponent reaches $\sim$ -1.

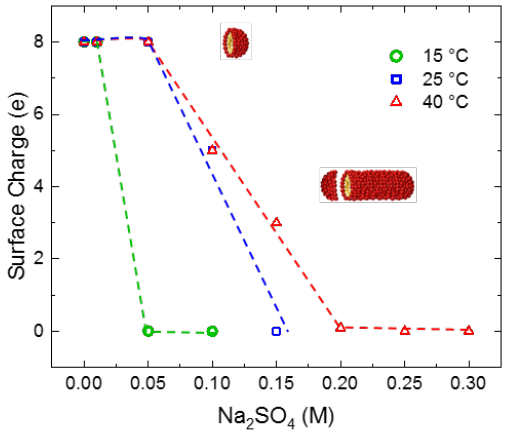

Figure S10. Micellar surface charge as function of salt concentration and temperature obtained by SANS data fitting. Charge screening increases with salt concentration causing the surface charge on each micelle to become less negative. A higher salt concentration is required to induce this effect at higher temperature.

7 SANS analysis of lamellar peak and associated precipitation

A Gaussian fit of the peak profiles at Q $\simeq$ 0.2 Å extracted from the SANS experiments carried out at 15 °C, reveals that initially the intensity of the Bragg peak I^* increases with salt concentration until a maximum value I_{max} is reached (Fig. S11a). Following this, the intensity decreases and nearly vanishes. Similar behaviour is observed at 25 °C, while at 40 °C the pattern is less obvious due to the postponed structural transformations for the range of added electrolyte at this temperature (Fig. S11a). The decrease in intensity of the Bragg peak is associated with the settling of the larger MLVs (100s nm) and clusters in surfactant-salt mixtures that can eventually be detected with the naked eye, as shown in the images of the sample in the right panel of Fig. S11b. The value of Q^* remains approximately constant as a function of salt addition and has a slight variation with temperature, which is however within the scatter of the data, likely associated with heterogeneity within the sample. This salting out effect has been documented in previous studies.[3] Fig. S11c indicates how the salt concentration at which I_{max} occurs changes with temperature. For T = 40 °C, no precipitation was found at 0.35 M salt, and thus the value of 0.4 M was selected as it corresponds to the highest concentration studied optically did not show precipitation. As the temperature increases, more salt is required to induce precipitation.

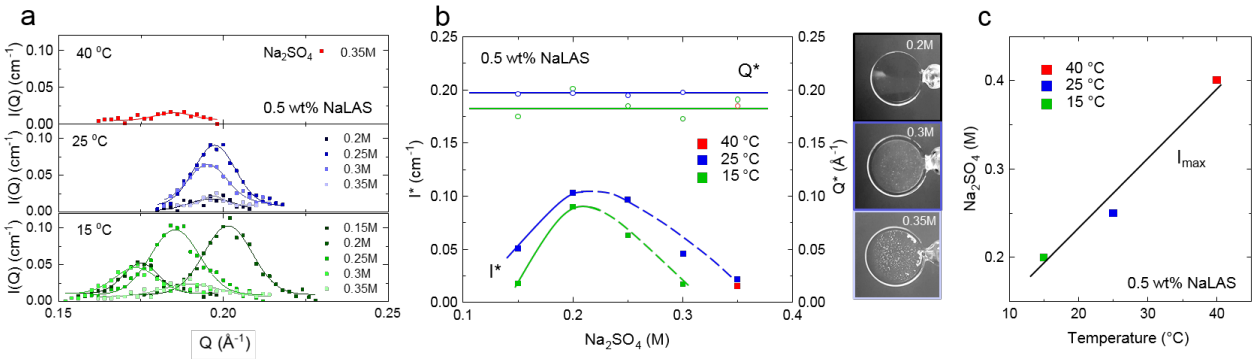

Figure S11. Analysis of the lamellar peak in experimental SANS data (corresponding to MLV formation) and the associated precipitation. (a) Gaussian profiles provide satisfactory model fits to the Bragg peak at all Na_2SO_4 concentrations and temperatures. (b) Dependence of the intensity I^* and location Q^* of each peak as a function of concentration and temperature. The additional images of the quartz cells used in the SANS experiment hold different concentrations of added salt (0.2-0.35 M). At a lower Na_2SO_4 concentration (0.2 M) the sample is clear, but with increasing concentration a visible precipitation is seen mirroring the fall in Bragg peak intensity. (c) Temperature dependence of the Na_2SO_4 concentration associated with the maximum Bragg peak intensity (I_{max}).

8 Additional cryo-TEM and optical microscopy images

Cryo-TEM and optical microscopy was used to complement the scattering data in real space in order to visualise the different NaLAS aggregates. Fig. S12 shows the various sizes of MLVs present within the 0.5 wt% NaLAS system with 0.2 M Na_2SO_4 added. The MLVs appear both in isolation and in clusters with a degree of polydispersity.

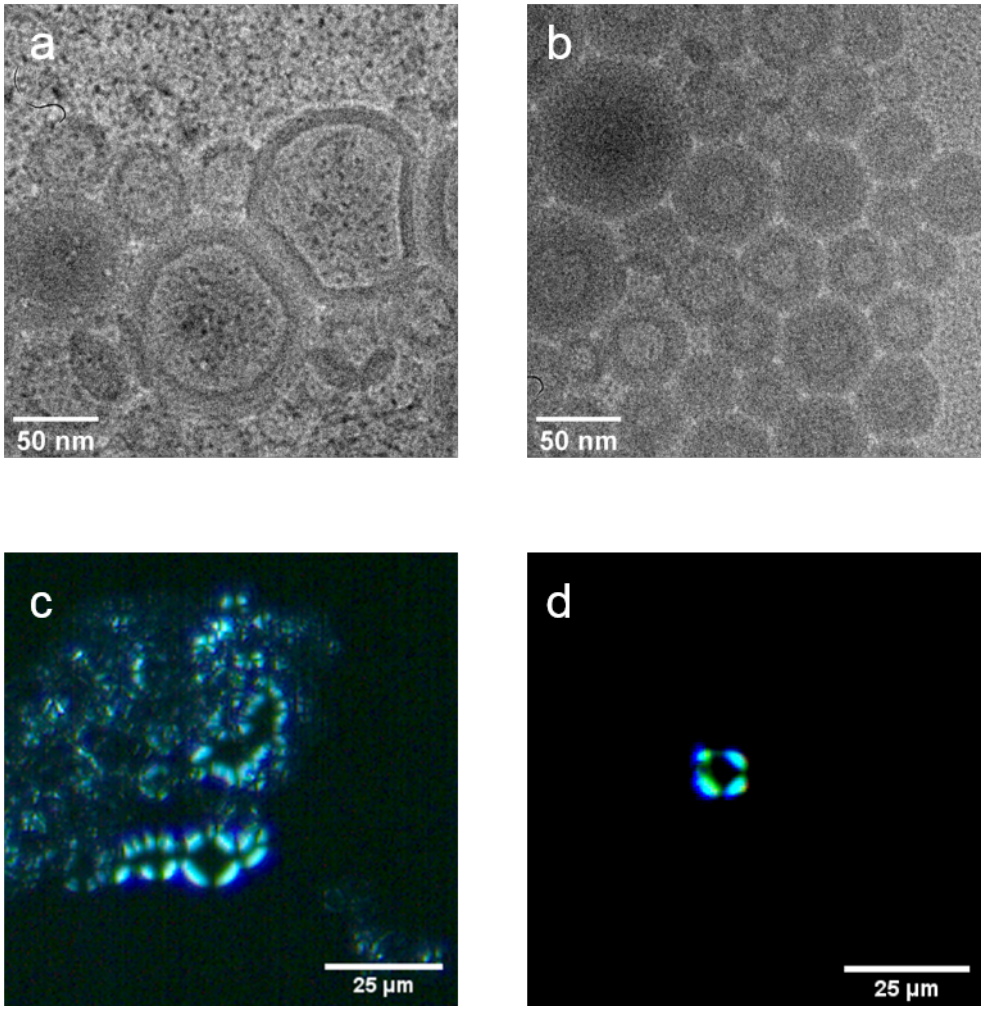

Figure S12. (a,b) Additional cryo-TEM images showing MLVs of different sizes taken from a sample of 0.5 wt% NaLAS with 0.2 M Na_2SO_4. (c,d) Optical microscopy images of the same system taken at 20 °C.

References

1. Tanford, C. Micelle shape and size. *J. Phys. Chem.* **76**, 3020–3024 (1972).
2. Hayter, J. & Penfold, J. Determination of micelle structure and charge by neutron small-angle scattering. *Colloid Polym. Sci.* **261**, 1022–1030 (1983).
3. Stewart, J., Saiani, A., Bayly, A. & Tiddy, G. Phase behavior of lyotropic liquid crystals in linear alkylbenzene sulphonate (las) systems in the presence of dilute and concentrated electrolyte. *J. Dispers. Sci. Technol.* **32**, 1700–1710 (2011).